

IN SITU CHARACTERIZATION OF ALKALI ANTIMONIDE PHOTOCATHODES*

J. Smedley, K. Attenkofer, S. G. Schubert, BNL, Upton, NY 11973, USA

H. A. Padmore, J. Wong, LBNL, Berkeley, CA 94720, USA

J. Xie, M. Demarteau, ANL, Argonne, IL 60439, USA

M. Ruiz-Oses, I. Ben-Zvi, X. Liang, E. M. Muller, Stony Brook University, Stony Brook, NY 11794, USA

A. Woll, Cornell University, Ithaca, NY 14850, USA

Abstract

Alkali antimonide photocathodes are a prime candidate for use in high-brightness photoinjectors of free electron lasers and 4th generation light sources. These materials have complex growth kinetics - many methods exist for forming the compounds, each photocathode having different grain size, roughness, and crystalline texture. These parameters impact the performance of the cathodes, including quantum efficiency (QE), intrinsic emittance and lifetime. In situ analysis of the growth of these materials has allowed investigation of correlations between the growth parameters and the resulting cathode performance. This work explores the relationship between the crystallinity of the initial antimony film and the roughness of the final cathode.

Two growth methods are compared – a “traditional” recipe which uses a crystalline initial antimony film and a “yo-yo” process which builds the cathode through an iterative process using sub-crystalline antimony layers. The traditional method provides exemplary QE (7.5% @ 532 nm), but an exceptionally rough surface. The “yo-yo” produces a somewhat lower final QE (4.9% @ 532 nm) but a much smoother surface, as observed by grazing incidence small angle x-ray scattering (GISAXS).

INTRODUCTION

While they provide high QE for visible light, and high average current operation in injectors [1-3], there is reason for significant concern that the intrinsic emittance of photoinjectors relying on alkali antimonide photocathodes may be impacted by the surface roughness of the cathode film [4]. Traditional growth methods have resulted in films that are very rough; atomic force microscopy (AFM) yields a 25 nm rms roughness (50% of the total film thickness) over a 100 nm spatial period [5]. This will particularly impact high-gradient injectors; an intrinsic emittance in excess of 1 $\mu\text{m}/\text{mm}$ is expected from this surface for a 20 MV/m emission field.

We have developed tools to understand the formation of these materials, both structurally and chemically, with the goal of altering the growth to produce cathodes with less roughness, better stoichiometry, and larger crystal grains. The in situ techniques being used are x-ray diffraction (XRD), grazing incidence small angle x-ray scattering (GISAXS) and x-ray reflection (XRR). These tools enable determination of the crystal form of the cathode at each phase of growth, the film thickness and roughness, the texture and grain size of the film, and the presence of

“imperfectly reacted” material. This work has been carried out at the National Synchrotron Light Source (NSLS) using beamline X21 and at the Cornell High Energy Synchrotron Source (CHESS) using beamline G3.

Here we focus on two cathodes; one grown using our typical “High QE” process, and a second grown with a “yo-yo” process that begins with an antimony layer that is not thick enough to have crystallized prior to the first layer of potassium being deposited. The rationale for this approach arises from the observed growth kinetics of the compound – the initial crystalline antimony layer is fully dissolved by the addition of potassium prior to forming an antimonide. The large variation in lattice constants likely leads to the formation of the observed rough surface structure, as the alkali initially diffuses along Sb grain boundaries and pushes the material apart, forming the observed nano-pillar structure [5]. By eliminating the crystalline Sb phase, we hope to prevent this roughening.

EXPERIMENT

In the interest of space, the growth chamber with in situ x-ray analysis is described elsewhere [6]. The cathodes were grown in a UHV chamber, with a typical operating pressure of 0.2 nTorr. Residual gas analysis confirms that the partial pressures of reactive gases (H_2O , CO) were better than 0.05 nTorr. Silicon [100] wafers $1 \times 2 \text{ cm}^2$ were used as substrates; these were exposed to HF prior to installation, and baked to 500 C for an hour prior to growth. Once the substrate has cooled to 160 C, a further cleaning of the substrate is achieved by an initial potassium evaporation – XRR measurements confirm that this K does not remain resident on the surface, however the QE of cathodes grown is significantly improved by this initial step. Antimony is evaporated from PtSb beads; alkali-Bi sources from Alvatech are used to supply Potassium and Cesium. Deposition is sequential, with Sb evaporated, then K, then Cs, all at $\sim 0.2 \text{ \AA}/\text{s}$. The QE is observed during K and Cs evaporation, and the deposition is halted when the QE reaches a plateau. The “traditional” cathode is a multi-layer growth on a single substrate, with the first cathode “baked off” (substrate raised to 500 C for 10 min) prior to the growth of a second.

1 st Layer	Tem p	QE	2 nd Layer	Temp	QE
15 nm Sb	100		15 nm Sb	125	
62 nm K	125	0.14	60 nm K	125	0.37
118 nm Cs	125	4.1	120 nm Cs	125	7.5

ISBN 978-3-95450-126-7

The “yo-yo” cathode is grown in two sequential steps, with no baking in between. The 3 nm initial Sb layer is below the crystallization threshold of 4 nm [5]. A further layer grown beyond this one did not improve the QE, suggesting that 8 nm of Sb results in a cathode sufficiently thick to efficiently absorb the 532 nm light.

1 st Layer	Tem	QE	2 nd Layer	Temp	QE
	p				
3 nm Sb	100		5 nm Sb	125	
12 nm K	125	0.16	16 nm K	125	0.88
42 nm Cs	125	3.1	44 nm Cs	125	4.9

RESULTS

X-ray Diffraction

Figure 1 shows the crystalline evolution of both cathodes after each growth step. For the traditional recipe, the initial Sb layer is a textured, crystalline film. After potassium is added, the film is a mix of K_2Sb and K_3Sb . After Cs is added, the cathode is cubic phase K_2CsSb with a 220 surface texture. The 500C bake (green dots) leaves an undetermined residual, which affects the crystalline evolution of the second cathode. The final state is again K_2CsSb with a 220 surface texture, but a significantly improved QE.

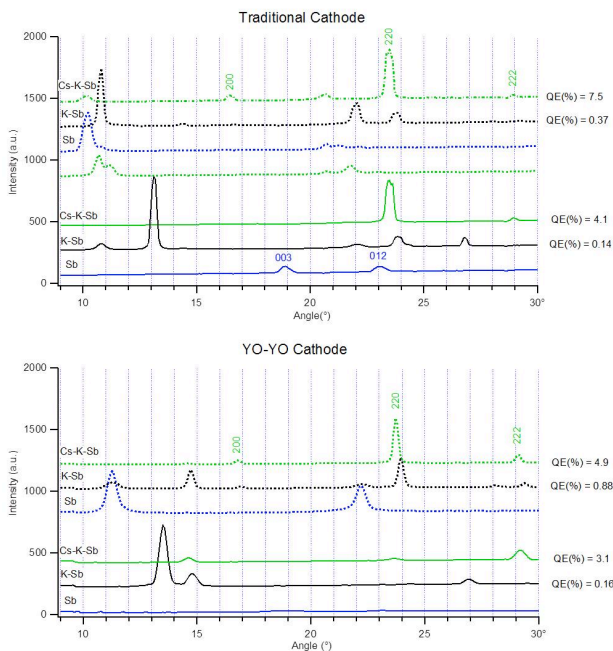


Figure 1: Crystalline evolution of cathodes grown by two different methods, observed via XRD. Scattering is out of the substrate plane, showing surface-normal textures.

The yo-yo recipe shows no crystalline structure after the initial Sb deposition, confirming that the layer is too thin to be crystalline. After K deposition, a mixed-phase potassium antimonide is observed, and after Cs deposition the cathode is not fully K_2CsSb . The second Sb step removes the QE, but does not correspond to crystalline Sb. The final state cathode is similar to that in the traditional recipe – a 220 textured K_2CsSb film.

ISBN 978-3-95450-126-7

X-ray Reflectivity

The variation of the intensity of the specular reflection from a surface as the x-ray angle of incidence is varied (for near-grazing angles) provides insight into the surface thickness and roughness of thin films if these films are sufficiently ordered to produce discernible interference patterns. This technique is called x-ray reflectivity (XRR), and has been used to measure the thickness of the films described above. Figure 2 shows the XRR data for the first deposition of the traditional recipe, along with the fit thickness and roughness from Parratt’s recursion [7] implemented in Matlab. It is important to note that the “roughness” measured in this manner is actually the variation in height of the nano-pillar structure – it is not the full roughness measured with an AFM on this discontinuous film, which includes the valleys between the pillars. The second layer was too rough for the XRR to provide a meaningful thickness or roughness measurement. Interestingly, the total thickness of this cathode did not increase during the first K deposition; the cause of this anomaly is under investigation.

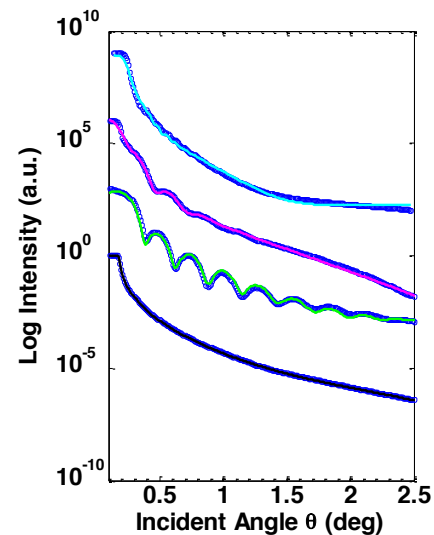


Figure 2: XRR for first deposition of traditional recipe. Curves, from the bottom: substrate, post Sb, post K, and post Cs. Best fit lines are shown (values in table below).

Deposited Layers	Total Thickness (Å)	Roughness (Å)
Cs-K-Sb/Si	473	23
K-Sb/Si	131	18
Sb/Si	130	4.6
Substrate	-	3.6

Figure 3 shows the XRR analysis for the yo-yo cathode. Here the analysis remains possible through both cathode depositions, suggesting that the final cathode is significantly smoother. It is interesting to note that the final cathode thickness (47 nm) is very similar to that of the first layer of the traditional cathode.

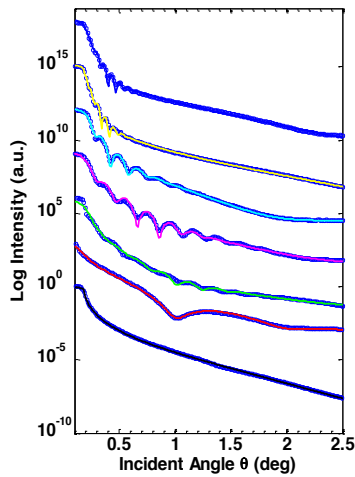


Figure 3: XRR for yo-yo recipe. The bottom curve is the substrate, with each additional layer shown in ascending order. Best fit lines are shown (values in table below).

Deposited Layers	Total Thickness (Å)	Roughness (Å)
Cs-K-Sb-Cs-K-Sb/Si	469	32
K-Sb-Cs-K-Sb/Si	449	36
Sb-Cs-K-Sb/Si	200	21.3
Cs-K-Sb/Si	174	13.2
K-Sb/Si	141	10.5
Sb/Si	35	2.9
Substrate	-	3.1

Grazing Incidence Small Angle X-ray Scattering

In addition to being reflected, x-rays are scattered from a surface based on the film surface structure. While XRR provides insight into the variation in height of the nano-pillars that make up the cathode, GISAXS permits the identification of lateral domains. In principle, GISAXS can be used to determine the lateral domain size, however for the purposes of the current work, the presence and intensity of a GISAXS pattern is used as a diagnostic of film roughness.

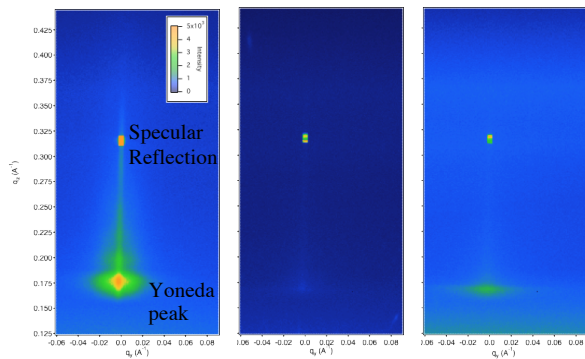


Figure 4: GISAXS of 1st cathode with 1.8° incidence angle. Post Sb on left, post K in center and post Cs on right. The 2nd layer was too rough to produce a pattern.

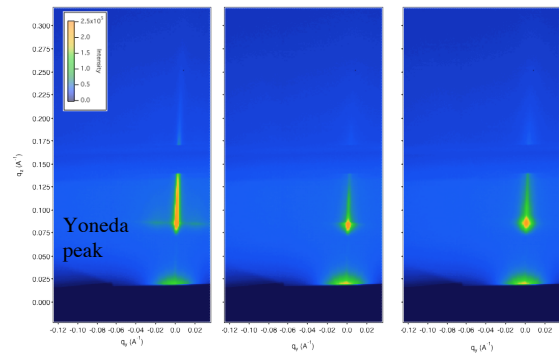
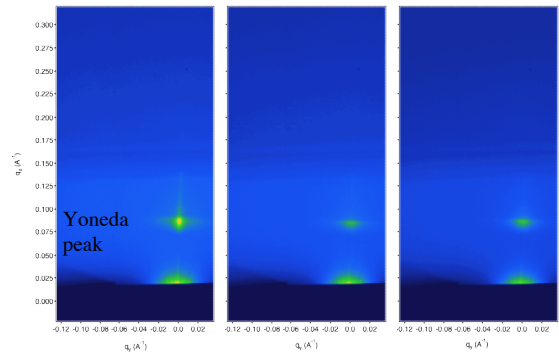


Figure 5: GISAXS of the yo-yo cathode. The specular peak is blocked to improve observation of the GISAXS pattern. The sequence proceeds from left to right: Sb, K, Cs. The 2nd deposition is shown below in the same order.



CONCLUSIONS

XRD, XRR and GISAXS have been used to observe the evolution of two bi-alkali cathodes grown on silicon substrates. The traditional recipe produces superior QE, yet exhibits a surface feature likely to lead to a strong field dependence of the intrinsic emittance. A variant iterative process beginning from a sub-crystalline Sb layer produces a somewhat lower QE, but a much smoother surface, and may be attractive for high brightness electron injectors.

This work was supported by the US DOE, under Contracts DE-AC02-05CH11231, DE-AC02-98CH10886, KC0407-ALSJNT-I0013, and DE-SC0005713. Use of CHSS is supported by NSF award DMR-0936384.

REFERENCES

- [1] L. Cultrera, et al, Phys. Rev. ST Accel. Beams 14, 120101 (2011)
- [2] R. R. Mammei, et al, Phys. Rev. ST - Accel. Beams 16, 033401 (2013)
- [3] T. Vecchione, et al, Appl. Phys. Lett. 99, 034103 (2011)
- [4] T. Vecchione, et al, Proceedings of IPAC2012, New Orleans, Louisiana, USA, 655 (2012)
- [5] S. G. Shubert, et al, accepted for publication in Appl. Phys. Lett. Mat. (2013)
- [6] J. Smedley, et al, Proceedings of IPAC2013, Shanghai, China, 464 (2013)
- [7] Parratt, L.G., Phys. Rev. 95, 359 (1954)